Available online at www.sciencedirect.com

ScienceDirect

Procedia Engineering 105 (2015) 346 – 358

Procedia Engineering

www.elsevier.com/locate/procedia

6th BSME International Conference on Thermal Engineering (ICTE 2014)

Stability of flow past alternate rigid and porous panels in boundary layer flow and in channel flow

A. R. Paul, P. K. Sen[1] and S. Hegde

Department of Applied Mechanics, Indian Institute of Technology Delhi, New Delhi 110-016, India.

Abstract

Propagation of two-dimensional small amplitude Tollmien-Schlichting (TS) waves has been investigated over a rigid panel followed by a porous panel in the presence of cross-flow. In the present work boundary layer flow over alternate rigid-porous panels in which suction is applied through the porous panel is investigated.Also investigated is the problem of flow past alternate rigid and porous panels with cross flow. A general space marching solution has been discussed for calculating the mean velocity profile for the above case, in the developing region of mean flow in the porous panel, following the rigid-porous junction. Numerical solutions are obtained using a finite difference method for the suitably simplified Navier Stokes equations, using appropriate boundary conditions.

Detailed two-dimensional analyses have been done for the disturbance waves using both the quasi-parallel (QP) approximation, and more accurately, using the non-parallel (NP) approach. The non-parallel approach has been carried out over the developing mean-flow region of the porous panel, following the rigid-porous junction.

Numerical solutions have been obtained by finite difference procedures. In some of the cases results have been validated with the available literature. Finally, the jumps in the amplitude of the disturbance waves across the rigid-porous junction were calculated using the theory of Sen *et al.*[6].

The important outcome from this work is in optimizing the length of the porous panel, following the rigid-porous junction. It is seen that, as compared to the length required to approach the asymptotic mean flow state to within 99%, only a very short porous panel length is sufficient to stabilize the disturbances.

Hence, it is foreseen that alternate long rigid panels, with in-between short porous panels, could be a very effective way of stabilizing the disturbances, and thus delaying laminar to turbulent transition.

Peer-review under responsibility of organizing committee of the 6th BSME International Conference on Thermal Engineering (ICTE 2014)

Keywords: Disturbance waves, rigid-porous panels, quasi-parallel, nonparallel, wave driver theory.

1. Introduction

It was observed in the past in boundary layer flows that suction can delay laminar to turbulent transition. Using wall suction in a flow, the turbulent state will not occur at its usually expected Reynolds numbers. This may have stabilizing effect on the flow disturbances. The stabilization occurs mainly because the

[1]Corresponding author, email:pksen@am.iitd.ac.in

Peer-review under responsibility of organizing committee of the 6th BSME International Conference on Thermal Engineering (ICTE 2014)
doi:10.1016/j.proeng.2015.05.015

mean velocity profile is altered in shape so that the flow is more stable to disturbances. Therefore, even if the disturbance is growing on the rigid side, there is a damping effect on the porous side when suction or suction cum injection is applied. A typical schematic view of disturbance propagation across the rigid-porous panels is shown in Figure 1. For the sake of simplicity only one Tollmien Schlichting (TS) wave is taken into consideration the amplitude of which is monitored along x.

The propagation of TS wave across a junction of alternate rigid-compliant panels in a channel flow has been studied by Carpenter and Sen [1]. They have shown good agreement between their results and those obtained from the direct numerical simulation (DNS) results of Davies and Carpenter [2]. The method developed by Sen *et al.* [3] is fairly generic, and, the same methodology is applied here across the junction between rigid and porous panels. Furthermore, Fransson and Alfredsson [4] have given the stability analysis for channel flow but they have not reported any porous developing region.

In the present exercise, propagating disturbance waves have been studied across the rigid panel joined to a porous panel for two different flow geometries, viz. (i) flow across a rigid-porous flat plate boundary layer with applied suction; and, (ii) flow through a rigid-porous plane channel flow with applied cross-flow. A general solution for mean velocity profile has been presented across the porous developing region. Stability analysis has been conducted over the developing region using QP and NP approaches. Amplitude jump has been calculated at the near discontinuity at the rigid porous junction. Finally, optimimal porous panel length has been calculated based on the cumulative decay of the disturbance.

2. Formulation of the problem

2.1. Description of mean flow - Boundary layer flow case

In the present study, the mean flow has been considered as steady, incompressible and Newtonian. The x co-ordinate is chosen along the direction of flow and y is normal to the horizontal plane.

A schematic arrangement of the rigid porous boundary-layer is shown in Figure 2, where the boundary-layer thickness, δ, is growing for the rigid wall and the mean velocity profile is Blasius (viz. 'BR' for "boundary layer rigid") solution. At the junction, the boundary layer thickness reaches its maximum value δ_0 and afterwards the applied suction is such that there will not be any change in the boundary layer *displacement thickness* δ_0^*. Immediately after the junction, the velocity transforms into first the "entry to porous boundary layer (EBP) profile" and afterwards"developing porous boundary layer (DBP) profile". This EBP profile has the Blasius velocity profile for the $\overline{u}$-component, with an additional constant cross-flow suction component $\overline{v}$. The uniform suction velocity is taken as $\overline{v} = -1/R$, where, R is based on the displacement thickness δ_0^* at the junction. Finally, the DBP profile approaches to the asymptotic suction (AS) velocity profile. The mean velocity profile for the DBP can be obtained from the generalized boundary layer equation and the AS region has its standard asymptotic profile.

2.2. Description of mean flow - Channel flow case

Next discussed is the channel flow case, the schematic arrangement for which is shown inf figure 2. In the present study, the rigid side flow is given by the well-known channel flow parabolic velocity profile CR (viz. ' CR' for "channel-rigid"). The rigid part is for $-L \leq x < 0$ and, the porous part is for $x > 0$. Unlike the boundary-layer case, the cross-flow Reynolds number R_w (defined subsequently) is kept as a parameter in the problem. The width of the channel is from $y = 0$, to $y = y_l$, with $y_l = 2H$, where H is the half-width of the channel, and is also the length scale of the problem. The velocity scale of the problem is the rigid-side channel centerline velocity U_0.

After the junction, the CR velocity profile, changes to first the "entry to porous channel flow" (ECP) profile and afterward the "developing porous channel flow" (DCP) region as shown in Figure 3. This ECP profile has the usual parabolic velocity profile for the $\overline{u}$-component across which a constant cross-flow velocity component, $\overline{v} = R_w/R$, is applied. Here, R_w, the cross flow Reynolds number, is defined as $R_w = VH/\nu$, and V is the dimensional cross-flow velocity and ν is the kinematic viscosity. Also, R is the flow Reynolds number of the problem defined as $R = U_0H/\nu$. The developing velocity profile, DCP, gradually

changes along the x-direction and eventually becomes the "asymptotic channel porous (ACP) flow" velocity profile.

The mean velocity profile for the DCP and ACP region can be obtained from the reduced form of the non-dimensional Navier Stokes equation given below:

$$\overline{u}\frac{\partial \overline{u}}{\partial x} + \overline{v}\frac{\partial \overline{u}}{\partial y} = -\frac{\partial}{\partial x}(\overline{p}_l + \overline{p}_c) + \frac{1}{R}\frac{\partial^2 \overline{u}}{\partial y^2} \quad . \tag{1}$$

where, $\overline{p}_l$ is the pressure when the flow is parallel, and $\overline{p}_c$ is the pressure correction term consequent upon mass flux remaining constant at every station in x.

2.3. Description of the disturbance equations

In the present investigation, the non-dimensional Navier Stokes equations for two-dimensional incompressible flow is used in terms of the stream function as follows:

$$\frac{\partial}{\partial t}\left(\nabla^2 \Psi_t\right) + \frac{\partial \Psi_t}{\partial y}\frac{\partial}{\partial x}\left(\nabla^2 \Psi_t\right) - \frac{\partial \Psi_t}{\partial x}\frac{\partial}{\partial y}\left(\nabla^2 \Psi_t\right) - \frac{1}{R}\left(\nabla^4 \Psi_t\right) = 0 \quad . \tag{2}$$

where Ψ_t is the total stream-function and can be expressed as the sum of a steady mean part, ψ_0, and, a time dependent disturbance part, ψ, of the form below:

$$\Psi_t = \psi_0(x,\, y) + \psi(x,\, y,\, t) \quad . \tag{3}$$

The stream-wise and the normal mean velocity components can be obtained from ψ_0 as follows:

$$\overline{u} = \frac{\partial \psi_0}{\partial y}; \quad \overline{v} = -\frac{\partial \psi_0}{\partial x} \quad . \tag{4}$$

where overbar $\bar{()}$ is the generic symbol for the mean part. After substituting eq. (3) in eq. (2), one needs to filter out the mean flow part. Thereafter, the linearized Navier Stokes equation may be obtained. The combined equation, prior to separating mean and disturbance parts, is given below:

$$\begin{aligned}\frac{\partial}{\partial t}\left(\nabla^2 \psi\right) + \left(\frac{\partial \psi_0}{\partial y} + \frac{\partial \psi}{\partial y}\right)\frac{\partial}{\partial x}\left(\nabla^2 \psi_0\right) + \frac{\partial \psi_0}{\partial y}\frac{\partial}{\partial x}\left(\nabla^2 \psi\right) - \left(\frac{\partial \psi_0}{\partial x} + \frac{\partial \psi}{\partial x}\right)\frac{\partial}{\partial y}\left(\nabla^2 \psi_0\right) \\ - \frac{\partial \psi_0}{\partial x}\frac{\partial}{\partial y}\left(\nabla^2 \psi\right) - \frac{1}{R}\left(\nabla^4 \psi\right) = 0 \quad .\end{aligned} \tag{5}$$

We note that in the eq. (5), the Reynolds number R is based on constant length scale. The disturbance stream-function ψ can in general be expressed in normal mode form as follows:

$$\psi(x,\, y,\, t) = \phi(x, y) e^{i[\int \alpha dx - \beta t]} \quad . \tag{6}$$

In the above, α is the spatial wave number, β is the temporal frequency and $c = \beta/\alpha$ is the phase speed. In the spatial problem β is held real, and, α is obtained as a complex eigenvalue. In the non-parallel problem the amplitude ϕ is a function of y and also a slowly varying function of x. Also, in the non-parallel problem $\alpha = \alpha(x)$ is a slowly varying function of x. In numerical work, the term $\partial\alpha/\partial x$ may be neglected since it is numerically small. Therefore, eq. (6) may be simplified and rewritten as follows:

$$\psi\,(x,\, y,\, t) = \phi(x, y) e^{i(\alpha x - \beta t)} \quad . \tag{7}$$

After substituting for the stream-function ψ from eq. (7), into eq. (5), and after some algebra, one obtains an extended form of the Orr-Sommerfeld equation given below:

$$\begin{aligned}i\alpha\left[(\overline{u} - c)\left(\phi'' - \alpha^2\phi\right) - \overline{u}''\phi\right] - \frac{1}{R}\left(\phi'''' - 2\alpha^2\phi'' + \alpha^4\phi\right) + \frac{\partial \overline{u}'}{\partial x}\phi' + \overline{v}\left(\phi''' - \alpha^2\phi'\right) \\ = -\left[\overline{u}\left(D^2 - \alpha^2\right) - 2\alpha^2\,(\overline{u} - c) - \overline{u}''\right]\frac{\partial \phi}{\partial x} \quad .\end{aligned} \tag{8}$$

where, $D = (\partial/\partial y)$. This is the general equation for any type of flow configuration, like rigid or porous boundary-layer flow, or, rigid or porous plane channel flow. The above form is based on normalisation using a fixed length scale.

2.3.1. Quasi-parallel approximation

For rigid wall boundary-layer flow and developing channel flow, or for developing porous wall mean flow, the mean non-dimensional velocity $\overline{u}$ is a function of the wall normal direction y, but it also has a weak dependence on x. In general therefore $\overline{u} = \overline{u}(x, y)$. However, in the quasi-parallel (QP) approximation a *local function* $\overline{u} = \overline{u}(y)$ is used at each respective station in x, and, $\partial\overline{u}/\partial x$ is set as zero. Hence, $\phi(x, y) \simeq \phi(y)$ at each station in x. Similarly, the mean velocity $\overline{v}$, which is $\overline{v} \sim O(1/R)$, is also neglected for the rigid wall (though not for the porous wall). Thus, again redefining the stream-function for the quasi-parallel approximation case, one can write it as follows:

$$\psi\,(x,\,y,\,t) = \phi(y)\,e^{i(\alpha x-\beta t)} \quad . \tag{9}$$

Substituting the stream-function ψ from eq. (9) in eq. (8) and neglecting the $\partial/\partial x \sim O(R^{-1})$ terms in the differential equation, the well known classical Orr-Sommerfeld equation is obtained as follows:

$$i\alpha[(\overline{u} - c)(\phi'' - \alpha^2\phi) - \overline{u}''\phi] - \frac{1}{R}(\phi'''' - 2\alpha^2\phi'' + \alpha^4\phi) \;=\; 0 \quad . \tag{10}$$

The equation (10) can be written in operator form as follows:

$$L_{OS}(\phi) = 0 \quad . \tag{11}$$

where, L_{OS} is the classical Orr-Sommerfeld operator. This homogeneous eq. (11) can be solved for a given $\overline{u}$. The equation is valid for region I as shown in Figures 1 and 2, as a quasi-parallel approximation of the rigid wall boundary-layer and channel flow respectively.

2.3.2. Modified Quasi-parallel approximation

In the case of quasi-parallel approach, for the case of porous part, though the order of magnitude of the normal $\overline{v}$ component is $O(R^{-1})$, one cannot neglect $\overline{v}$ because the wall velocity $\overline{v}_w$, through the porous wall, is an important parameter. The modified Orr-Sommerfeld equation, after retaining $\overline{v}_w$ for the porous wall region, is obtained as follows:

$$i\alpha[(\overline{u} - c)(\phi'' - \alpha^2\phi) - \overline{u}''\phi] + \overline{v}(\phi''' - \alpha^2\phi') - \frac{1}{R}(\phi'''' - 2\alpha^2\phi'' + \alpha^4\phi) = 0 \quad , \tag{12}$$

where $\overline{v} \simeq \overline{v}_w = -\frac{1}{R}$ for boundary layer flow $\overline{v} \simeq \overline{v}_w = \frac{R_w}{R}$ for channel flow. Equation (12) can be written in operator form as follows:

$$L_{OP}(\phi) = 0 \quad . \tag{13}$$

where, L_{OP} is the extended Orr-Sommerfeld operator for the porous side. The homogeneous solution of eq. (13) is applicable for region III of Figure 1.

2.3.3. Developing flow region on a porous wall

As mentioned before, for the porous developing region the suction velocity is so chosen that the boundary-layer displacement thickness remains constant until the velocity profile fully transforms into the asymptotic suction profile. Defining, the displacement thickness δ_0^* as the length scale, and, the free stream velocity U_∞ as the velocity scale, the Orr-Sommerfeld equation (8) can be rewritten in operator form as follows:

$$(L_{OP} + L_{NP})\phi = L_2\left(\frac{\partial\phi}{\partial x}\right)_y \tag{14}$$

where, L_{OP} is the extended Orr-Sommerfeld operator vide eqs. (13). The nonparallel operator L_{NP} for the porous side and the operator L_2 are respectively as follows:

$$L_{NP} = \left(\frac{\partial\overline{u}'}{\partial x}\right)D; \;\; L_2 = [\overline{u}(D^2 - \alpha^2) - 2\alpha^2(\overline{u} - c) - \overline{u}''] \tag{15}$$

The homogeneous equation corresponding to eq. (14) is:

$$(L_{OP} + L_{NP})\phi = 0 \quad \text{or,} \quad L_{TP}\phi = 0 \tag{16}$$

where, the total operator L_{TP} corresponds to the operator inclusive of nonparallel effects for the porous wall. The homogeneous equation eq. (16) can be solved separately with the proper boundary conditions described below for the porous boundary layer flow and channel flow.

The full eq. (14) is solved using a procedure described in a companion paper by Sen et al [5]. The jump in the amplitude at the rigid-porous junction is calculated by using a procedure discussed by Sen et al [3].

2.4. Boundary conditions

We will now look into the boundary conditions for both walls, viz. rigid and porous walls, where the disturbance eqs. (11), (13) and (16) respectively are valid.

The disturbance velocities in the stream-wise and normal direction are respectively zero at the rigid wall . Thus, the boundary conditions for the rigid wall boundary layer flow is ,

$$\text{at the wall,} \quad y = 0; \quad \phi, \phi' = 0 \tag{17}$$

$$\text{at the outer boundary,} \quad y_l \geq 3; \quad \phi \approx e^{-\alpha y} \tag{18}$$

where y is normalised based on the displacement thickness.

In case of channel flow problem, the full width of the channel section has to be considered as the flow domain. Hence,

$$\text{at the lower wall,} \quad y = 0; \quad \phi, \phi' = 0 \tag{19}$$

$$\text{at the upper wall,} \quad y = y_l; \quad \phi, \phi' = 0 \tag{20}$$

In the present problem we consider small amplitude disturbances. For such disturbances the porous wall behaves like a rigid wall, since small pores are distributed all over it. Hence the boundary conditions are the same as above for porous boundary layer and channel flow respectively.

3. Results and discussions

Studies on propagating disturbance waves across a rigid plate joined to a porous plate have been carried out for two different flow geometries, viz. (i) flow across a rigid-porous flat plate boundary layer with applied suction; and, (ii) flow through a rigid-porous plane channel with applied cross-flow.

3.1. Rigid-Porous boundary layer flow with suction

Numerical results for boundary layer flow are given for Reynolds number, $R = 800$ (based on the displacement thickness δ^*). This value of 'R' pertains to the rigid-wall Reynolds number at the junction. For the porous side, R remains constant because the length scale is kept constant as δ_0^*, where δ_0^* is the value of δ^* at the junction. The rigid-side flow has been referred to as 'BR' , corresponding to Region I in sketch Figure 1. The velocity profile corresponding to the developing region in the porous plate, following the junction, is shown in Figure 4. In Figure 4 the terms 'EBP' , 'DBP' and 'AS' are defined corresponding to the developing flow region in the porous side as shown in Figure 2.

Variation in the root mean squared (r.m.s) values, of the fluctuating $u-$velocity $\hat{u}$ are shown in Figure 5. The profiles are normalised using the respective maximum values of $\hat{u}$. Also, figure 5 shows the $\hat{u}$ profile at $x = 0$ with and without suction, and near the AS state ($x = 8000$). These results are in very good agreement with those obtained by Fransson [6].

The spatial development of α_i, along the porous developing region, is shown in Figures 6. The growing disturbance, with constant frequency $F = 125$ and $R = 800$, has travelled over the rigid panel and finally reached the junction with the eigenvalue, $\alpha = 0.27258 - 0.005380i$. After the junction, due to the cross-flow suction component the eigenvalue experiences a jump for the EBP profile, i.e. $\alpha = 0.27828 - 0.003283$.

Along the porous panel α_i reduces very fast initially and attains a minimum value. Thereafter α_i increases and eventually reaches a constant value as the AS state is approached.

The results for α_i, based on QP and NP, are also presented in Figure 6. The differences in α_i, for QP and NP, are clearly visible in Figures 6a,b . For the porous wall case it is clear from Figure 6b that initially, i.e. for ($x < 350$), there is a substantial difference in α_i using the two approaches, viz. QP and NP. Thereafter, as the flow progresses along x both the values of α_i approach each other. This is highlighted in Figure 6a.

Logarithmic cumulative growth rate of the disturbance amplitude $A(x)$, viz. $ln(A/A_0)$ has been calculated over the rigid boundary layer, with constant frequency $F = 125$ and with $A_0 = A(x)$ for $x = -80$. This is seen in Figure 7a, using QP and NP respectively. Some difference does arise in the value of $A(x)$ at the rigid-porous junction due to a slight jump at the junction. Just after the junction, the disturbance cumulative amplitude decays very fast as shown in Figure 7b though the velocity profile is not fully transformed into the asymptotic suction profile. In fact the disturbance cumulative amplitude decays by 2-logs within nearly 0.5% of the 'total porous length' of $x = 8000$, as shown in Figure 7b. Both the approaches, viz. QP and NP, qualitatively look similar to each other, though there are some differences as one moves along x. Thus one should choose the NP approach, rather than the QP approach, if greater accuracy is required at the initial stages.

From Figure 6, it is to be noted that α has attained 90% of the value at the AS state already at $x = 200$ i.e. at 2.5% of the porous panel length after the junction. The mean velocity profile approaches the AS velocity profile, to within 10^{-2} accuracy, around $x \simeq 1650$, and to within 10^{-3} accuracy, around $x \simeq 8000$. Hence $x = 8000$ is called the 'porous length'. Thus, from the engineering point of view, the initial porous panel length is very important as it has the most significant effect on the eigenvalue, as it approaches the AS state. However, for numerical interests one has to move further along the porous panel so that the eigenvalues match with the exact solution of the asymptotic suction profile. Numerically it has been seen that at $x = 8000$ the eigenvalue reaches $\alpha = 0.27484 + 0.055980i$ which closely matches with the exact eigenvalue for the AS suction profile i.e. $\alpha = 0.27490 + 0.056023i$.

3.2. Rigid-Porous plane channel flow with cross-flow

This section describes the rigid the porous channel flow problem. In channel flow, the rigid side parabolic mean velocity profile approaches the asymptotic mean flow profile in the porous sides, with applied cross-flow through the porous panel. Numerical results have been obtained based on the Reynolds number, $R = 12000$. The spatial marching mean velocity profiles at various stations along the developing porous region is shown in Figure 8 for constant cross-flow velocity $R_w = 2$.

Similar analysis for jumps, as for the boundary layer case, is carried out for channel flow case at the rigid-porous junction, for constant frequency, F. It is interesting to note that for channel flow, the jump at the junction becomes almost constant irrespective of whether the disturbance wave is damped, amplified or neutral, even though the flow Reynolds number is increasing.

As has already been discussed, in the channel case, R_w is a controlling parameter, and a slight change in the R_w causes a corresponding change in the mean velocity profile. Keeping the flow Reynolds number R constant at 12000, the jump has been calculated for several cross-flow R_w, with constant non-dimensional frequency $F = 20$. It is noteworthy that as the cross-flow Reynolds number increases from 2 to 10 the amplitude jump increases from $0.5 - 5\%$.

Variation in the root mean squared (r.m.s) values, of the fluctuating $u-$velocity, $\hat{u}$ velocity are shown in Figure 9. The profiles are normalised using the maximum value of $\hat{u}$.

The differences in α_i, for QP and NP, are clearly visible in Figure 10a,b . For the porous wall case it is clear from the Figure 10b that initially i.e. for ($x < 150$), there is a substantial difference in α_i using the two approaches, viz. QP and NP. Thereafter, as the flow progresses along x both the values of α_i approach each other. This is highlighted in Figure 10a.

Logarithmic cumulative growth rate of the disturbance amplitude $A(x)$, viz. $ln(A/A_0)$ has been calculated and is shown Figure 11 using QP and NP respectively. Some difference does arise in the value of $A(x)$ at the rigid-porous junction due to a slight jump at the junction. Just after the junction, the disturbance cumulative amplitude decays very fast as shown in Figure 11b though the velocity profile is not fully transformed into

the asymptotic suction profile. In fact the disturbance cumulative amplitude decays by 2logs within nearly 12.5% of the 'total porous length' of $x = 3820$. Both the approaches, viz. QP and NP, qualitatively look similar to each other, though there are some differences as one moves along x. Thus one should choose the NP approach, rather than the QP approach, if greater accuracy is required at the initial stages.

It has been seen that cross-flow has a stabilizing effect over boundary layer flow (I) and channel flow as well. It is also noted for porous channel flow that, not for all R_w, but for a band of R_w between 0.6 to 15, the flow can be controlled and kept stable. In fact the optimal R_w for stabilization is between $R_w = 2-4$. This is because though decay has started from $R_w = 0.6$ but the required porous length is minimum at $R_w = 4$, for the logarithmic cumulative disturbance amplitude to decay by 2-logs (10^{-2}). From $R_w = 5$ onwards though the logarithmic cumulative disturbance amplitude pattern looks qualitatively similar for $R_w \leq 4$. The porous length required to decay the disturbance by 2-logs (10^{-2}) starts increasing. This is because of the existence of a prominent point of inflexion in the mean velocity profile for $R_w \geq 5$. Also, higher cross flow is needed, higher the value of R_w. Hence results are given for $R_w = 2$, rather than $R_w = 4$.

4. Conclusions

4.1. Boundarylayer Flow

An alternate rigid-porous combination seems to be a good choice for transition control instead of a long porous panel. Now the question is what is an optimum porous panel length? A rough estimate of the approximate porous panel length can be obtained in the following manner. Assume hypothetically that the rigid wall were to continue beyond the rigid-porous junction. Then for the boundary layer case, the parameters at the junction are $[R, F] = [800, 125]$, and $\alpha_i = -0.005380$. Using that value of α_i it is seen that the cumulative disturbance amplitude would *increase* by 2-logs(10^2) for $x \simeq 850$. Whereas, if we replace the same rigid panel by porous panel, then, the cumulative disturbance amplitude *decays* by 2-logs(10^{-2}) within $x \simeq 150$.

4.2. Plane Channel Flow

For porous channel flow, using suction cum injection (suction and injection respectively from opposite walls), the mean velocity profile becomes asymmetric with respect to the channel centerline. Also with higher cross-flow Reynolds numbers ($R_w > 10$), the mean velocity profile becomes almost linear like plane Couette flow.

In the plane channel case, as cross-flow Reynolds number is a controlling parameter, it has been seen that even small values of R_w lead to a very rapid increase in the critical Reynolds number, as R_w increases.

After the rigid-porous junction the eigenvalues (imaginary part, α_i) along the porous developing region are numerically different using the QP approximation and NP approaches. However, the nature of the curves are similar using the two approaches, and, both sets converge to a common value as the asymptotic state is approached.

Substantial amplitude decay takes place within a short distane of the porous panel length, compared to the distance requiredd to reach the asymptotic mean flow state, to within 10^{-3} accuracy.

Hence, it is foreseen that alternate long rigid panels, with in-between short porous panels, could be a very effective way of stabilizing the disturbances, and thus delaying laminar to turbulent transition.

References

[1] Carpenter, P. W. & Sen, P. K. 2003, Propagation of waves across junctions between rigid and compliant walls. *IUTAM Symposium on Flow past highly compliant boundaries and in collapsible tubes*, University of Warwick, U.K.

[2] Davis, C. & Carpenter, P. W. 1997 Numerical simulation of the evolution of Tollmien-Schlichting waves over finite compliant panels. *J. Fluid Mech.* **336**, 361-392.

[3] Sen, P. K., Carpenter, P. W., Hegde, S. & Davies, C. 2009, A Wave driver theory for vortical waves propagating across junctions with application to those between rigid and compliant walls. *J. Fluid Mech.*, **625**, 1-46.

[4] Fransson, J. H. M., Alfredsson, P. H. 2003, On the hydrodynamic stability of channel flow with cross flow, *J. Fluid Mech.*, **482**, 51-90.

[5] Sen, P. K., Hegde, S. & Paul, A. R. 2015, Stability of disturbance waves in developing shear flows: A review of 'ad-hoc' methods , *6th BSME International Conference on Thermal Engineering (ICTE 2014 (Accepted for publication)*.
[6] Fransson J. H. M. 2001, Investigation of the asymptotic suction boundary layer, Lic. Thesis, KTH Stockholm, Sweden.

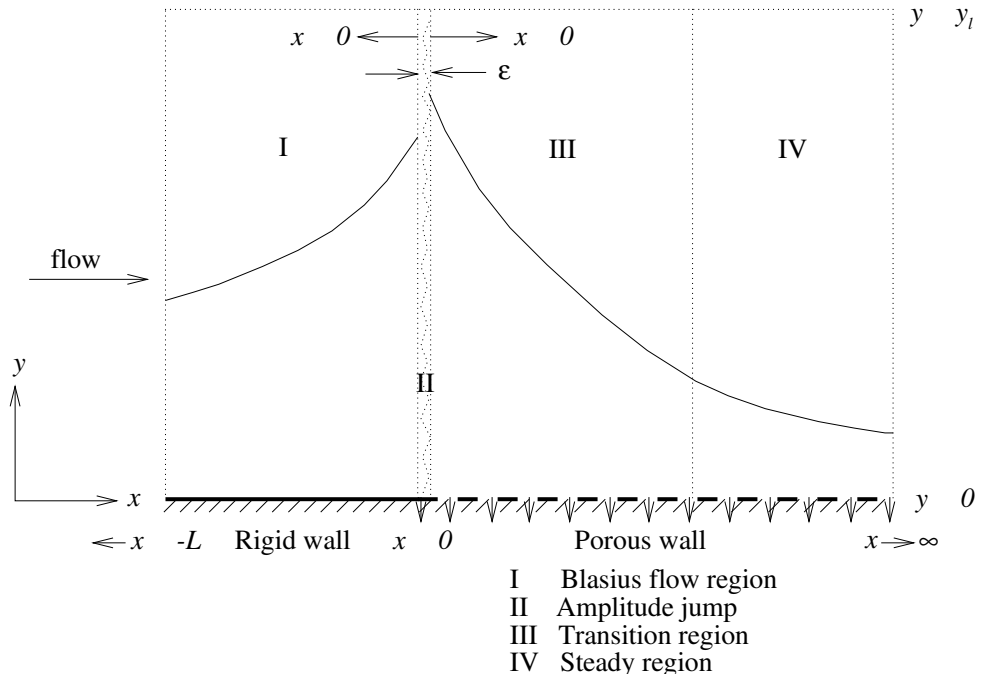

Fig. 1. Visualization of disturbance propagation over boundary layer flow with uniform suction

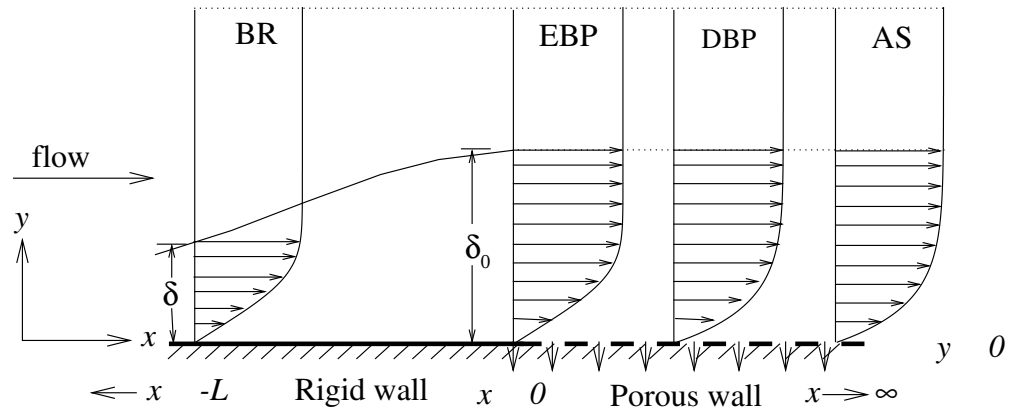

Fig. 2. Schematic diagram of boundary layer flow over rigid-porous plate with uniform suction

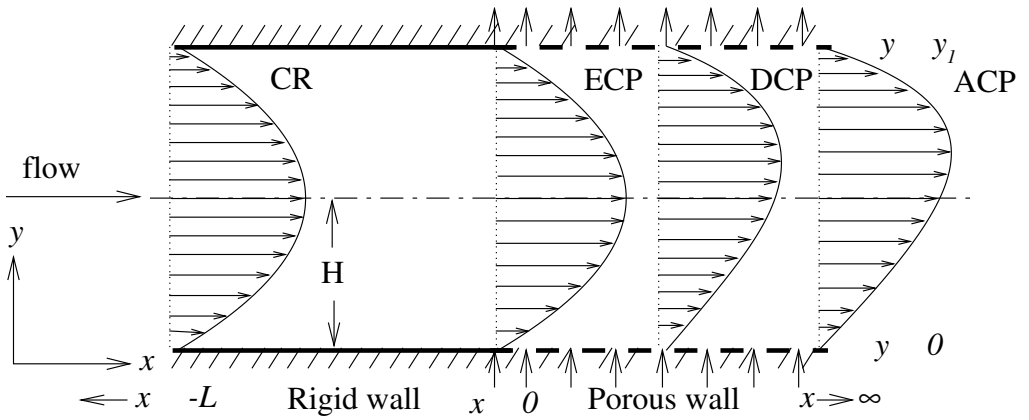

Fig. 3. Schematic diagram of flow through a channel with uniform suction-cum-injection

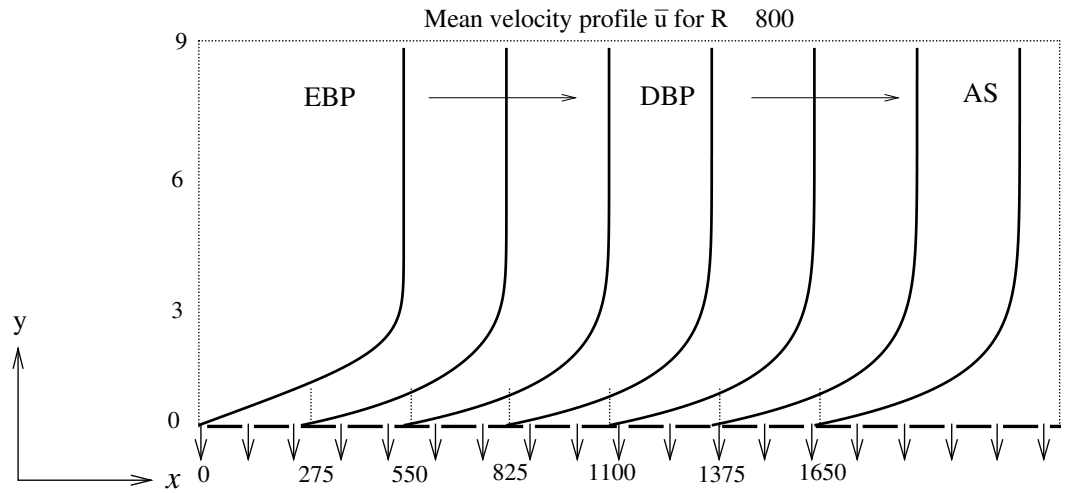

Fig. 4. Calculated mean velocity for developing porous region from the EBP to the AS profile, with uniform suction, for boundary layer flow

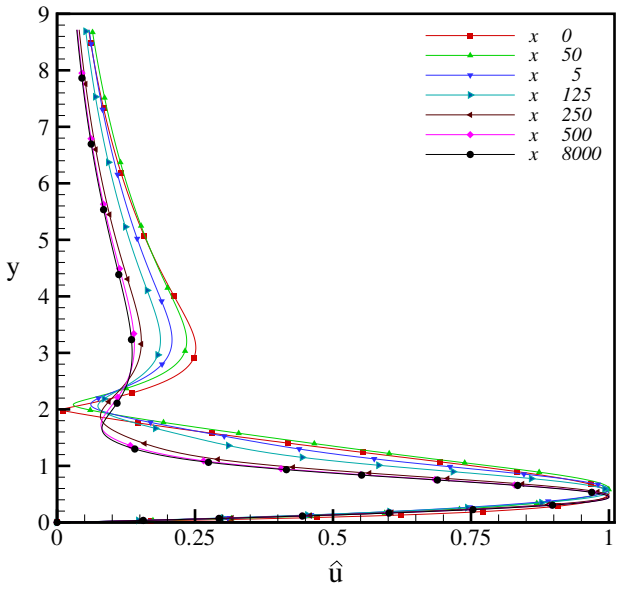

Fig. 5. Eigenfunctions of the $\hat{u}$-component normalized with its r.m.s. maximum value for the porous developing region from ($0 \leq x \leq 8000$) for boundary layer flow at $[R, F] = [800, 125]$

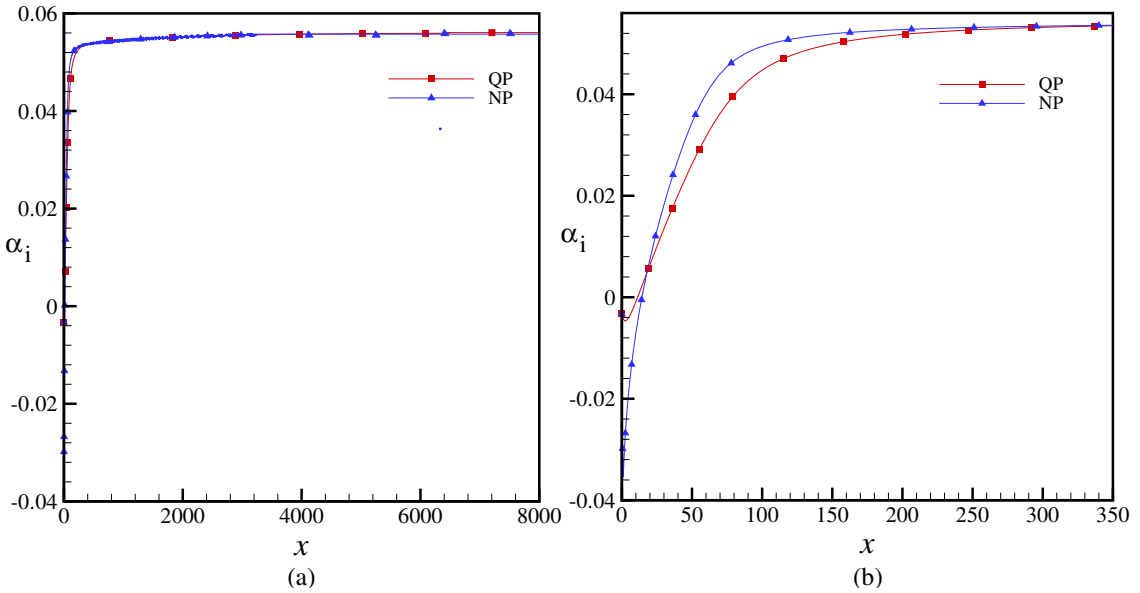

Fig. 6. Eigenvalue, α_i, along the porous developing region at $[R, F] = [800, 125]$; (a) Overall view from ($0 \leq x \leq 8000$) (b) Detail in the range of ($0 \leq x \leq 350$), using quasi-parallel (QP) and non-parallel (NP) approaches

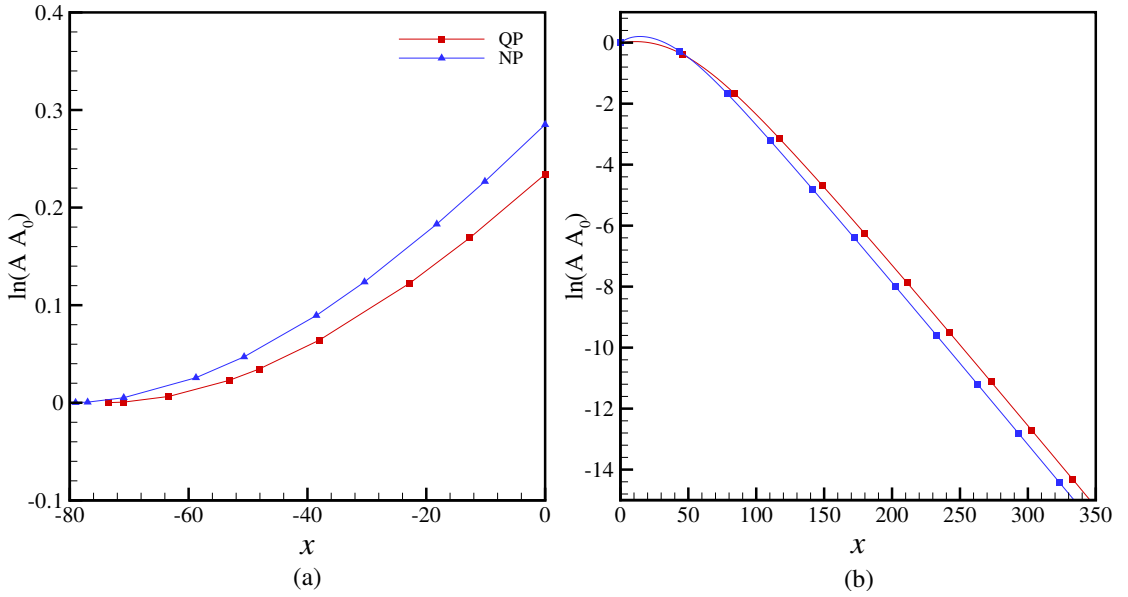

Fig. 7. Logarithmic amplitude growth-decay along boundary layer flow at $[R, F] = [800, 125]$; (a) rigid panel (b) porous panel, using quasi-parallel (QP) and non-parallel (NP) approaches

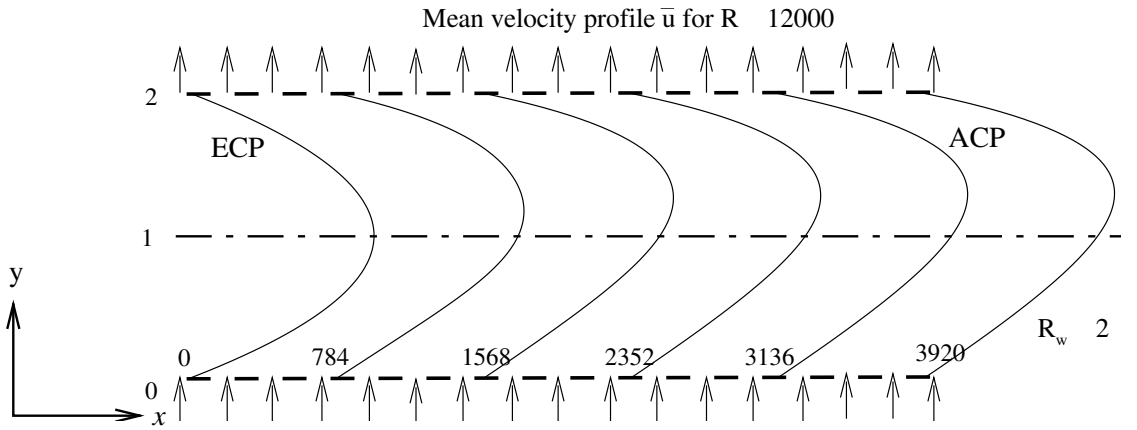

Fig. 8. Calculated mean velocity for disturbance region from the ECP to the ACP profile, with uniform cross-flow, $R_w = 2$, for channel flow

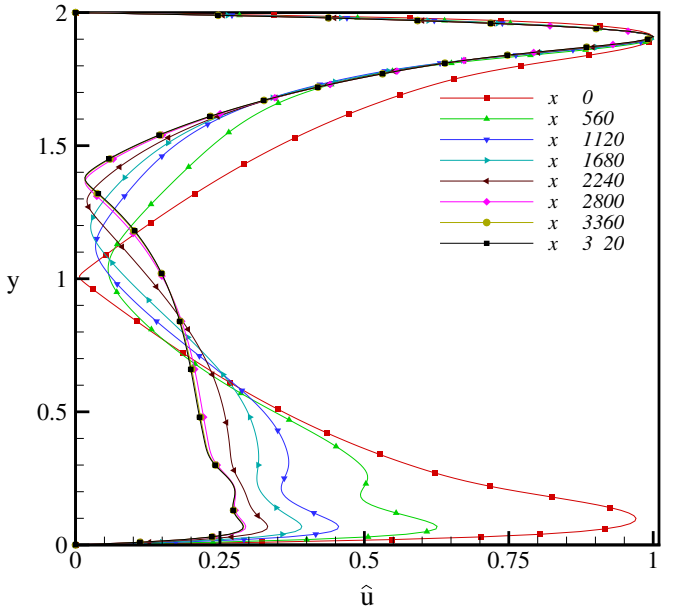

Fig. 9. Eigenfunctions of the $\hat{u}$-component normalized with its r.m.s. maximum value for the porous developing region from ($0 \leq x \leq 3920$) for channel flow at $[R, F] = [12000, 20]$, $R_w = 2$

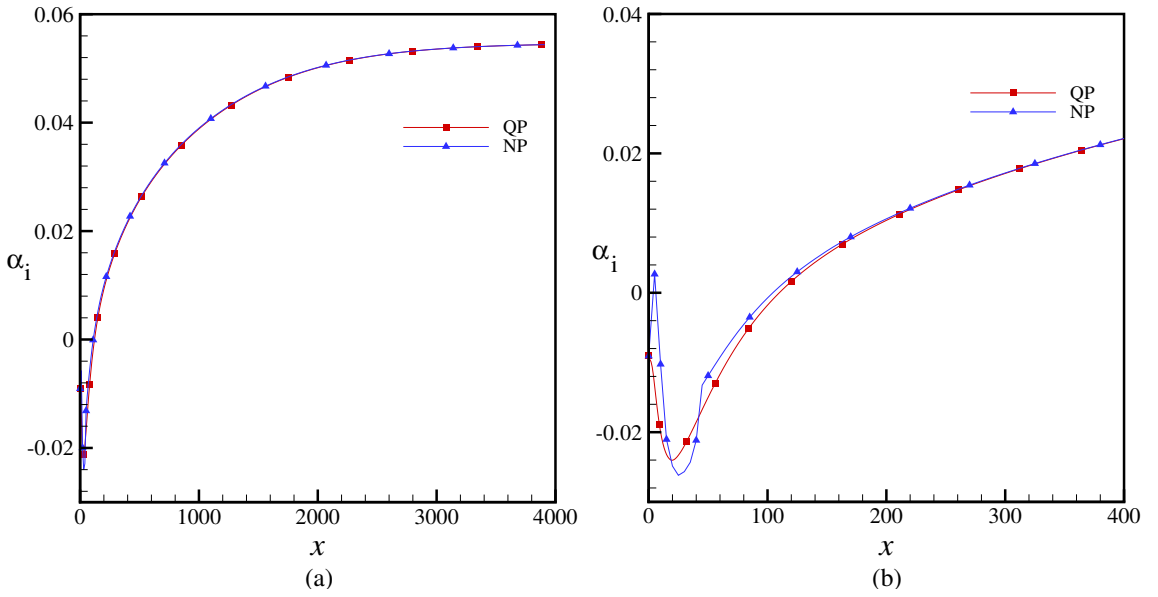

Fig. 10. Eigenvalue, α_i, along the porous developing region at $[R, F] = [12000, 20]$; (a) Overall view from ($0 \leq x \leq 3920$) (b) Detail in the range of ($0 \leq x \leq 400$), using quasi-parallel (QP) and non-parallel (NP) approaches. Results for $R_w = 2$

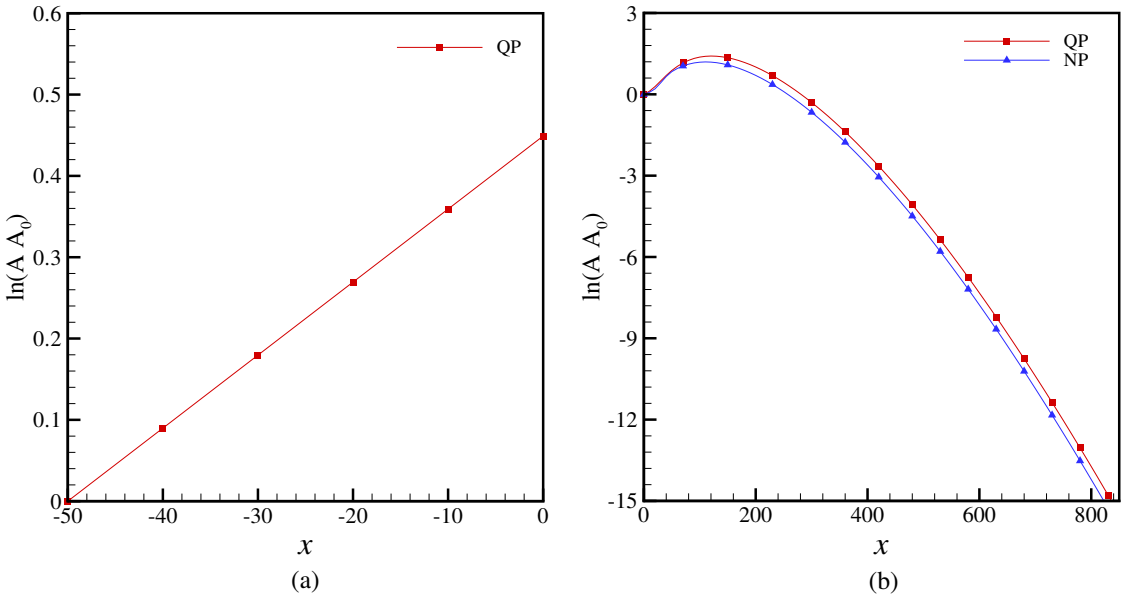

Fig. 11. Logarithmic amplitude growth-decay along channel flow at $[R, F] = [12000, 20]$; (a) rigid panel (b) porous panel, using quasi-parallel (QP) and non-parallel (NP) approaches. Results for $R_w = 2$